Climatology of ionospheric scintillation over the Vietnam low-latitude region for the period 2006-2014

Tran Thi Lan, Le Huy Minh, Christine Amory-Mazaudier, Rolland Fleury

Climatology of ionospheric scintillation over the Vietnam low-latitude region for the period 2006-2014

Tran Thi Lan[1], Le Huy Minh[1], C. Amory-Mazaudier[2,3], R. Fleury[4]

[1]*Institute of Geophysics, VAST, Cau Giay, Hanoi, VIETNAM*

[2]*Sorbonne Universités, UPMC Univ. Paris 06, UMR 7648, Laboratoire de Physique des Plasmas, F-75005, Paris, France*

[3]*T/ICT4D, ICTP, International Centre for Theoretical Physics, StradaCostiera, 11, I- 34151 Trieste Italy*

[4]*LAB-STICC,UMR6285, Institut Mines-Telecom Atlantique, CS 83818, 29288 Brest Cédex 3, France*

Correspondence to: T. T. Lan (lanttigp@gmail.com)

Abstract

This paper presents the characteristics of the occurrence of ionospheric scintillations at low-latitude, over Vietnam, by using continuous data of three GSV4004 receivers located at PHUT/Hanoï (105.9° E, 21.0° N; magnetic latitude 14.4° N), HUES/Hue (107.6° E, 16.5° N; magnetic latitude 9.5° N) and HOCM/ Ho Chi Minh city (106.6° E, 10.8° N; magnetic latitude 3.3° N) for the period 2006-2014. The results show that the scintillation activity is maximum during equinox months for all the years and depends on solar activity as expected. The correlations between the monthly percentage scintillation occurrence and the F10.7 flux are of 0.40, 0.52 and 0.67 for PHUT, HUES and HOCM respectively. The distribution of scintillation occurrences is dominant in the pre-midnight sector and around the northern crest of the equatorial ionization anomaly (EIA), from the 15°N to 20°N geographic latitude with a maximum at 16°N. The results obtained from the directional analysis show higher distributions of scintillations in the southern sky of PHUT and in the northern sky of HUES and HOCM, and in the elevation angles smaller than 40°. The correlation between ROTI and S_4 is low and

rather good at PHUT (under EIA) than HOCM (near equator). We found better correlation in the post-midnight hours and less correlation in the pre-midnight hours for all stations. When all satellites are considered during the period of 2009-2011, the range of variation of the ration between ROTI and S_4 is from 1 to 7 for PHUT, from 0.3 to 6 for HUES and from 0.7 to 6 for HOCM.

Keywords: Equatorial ionosphere, scintillation, ionospheric irregularities.

1. Introduction

The existence of equatorial plasma bubbles (EPB) is attributed to the instability of the Rayleigh-Taylor (R-T) plasma (Kelley, 2009 and references therein). The instability of the Rayleigh-Taylor plasma is triggered by the intensification of the eastward equatorial electric field just before its reversal, this intensification is called the Pre Reversal Enhancement (PRE). At the time of the PRE, the electric field oriented towards the east rapidly raises the ionospheric layers and creates large gradients of electronic density which is a condition for the development of R-T instability. The R-T instability mechanism is considered the primary mechanism responsible for the generation of ionospheric plasma density irregularities or plasma bubble in equatorial and low-latitude region (Maruyama, 2002; Rama Rao et al., 2006; Fejer et al., 1999). The plasma bubbles have typical east-west dimensions of several hundred kilometers, these contain irregularities with scale-lengths ranging from tens of kilometers to tens of centimeters (Tsunoda, 1980), extending along the geomagnetic field lines to the latitudes of the anomaly crest regions. These irregularities affect the propagation of electromagnetic waves and cause scintillations on the Global Positioning System (GPS) signal (Basu and Basu, 1981). The amplitude and phase of a radio signal crossing a region of irregularities in electronic ionospheric density are modified. The irregularities with size comparable or smaller than the first Fresnel zone ($D = \sqrt{2\lambda z}$, where D is the scale size of the irregularity, λ is the radio wavelength,

and z is the altitude of the irregularity layer) can cause scintillation in the GPS signal (Yeh and Liu, 1982). So far, the ionospheric scintillations associated with ionospheric irregularities remains a major subject regarding the space weather effects on trans-ionospheric signal propagation systems, such as the global positioning system (GPS), particularly at equatorial and low-latitude regions.

There are number of studies which reported climatology of GPS ionospheric scintillation and ionospheric irregularities activity from the GPS phase fluctuations in the different latitude regions (Pi et. al., 1997; Basu et al., 1999; Valladares et al., (2004); Rama Rao et al., 2006; Spogli et al., 2009; Beniguel et al., 2009; Alfonsi et al., 2013; etc.). Pi et al. (1997) have defined a ROTI index, based on the standard deviation of the rate of change of total electron content (TEC) over a 5-min period to monitor the ionospheric irregularities from the GPS phase fluctuations. Rama Rao et al. (2006) showed the spatial and temporal characteristics of L-band over Indian with the scintillation activity is stronger around the equatorial ionization anomaly (EIA) region and these scintillations are often accompanied by the TEC depletions scintillations over the Indian. Valladares et al. (2004) found out the anomaly crests are the regions where the most intense GPS scintillations and the deepest TEC depletions are encountered in South America. Recently, Abadi et al. (2014) investigated ionospheric scintillations for Indonesia low-latitude region and showed the characteristics of GPS scintillation associated with low-latitude ionospheric disturbances. Huang et al. (2014) reported GPS ionospheric scintillation during the phase of rising solar activity from 2010 to 2014 for the low latitude station of Shenzhen (China). In addition, several researchers have used TEC fluctuations (ROTI) to compare with amplitude scintillation (S_4 index) in low-latitude region. By comparing amplitude scintillations (S_4) with TEC fluctuations, Beach and Kintner (1999) concluded that the S_4 index is roughly proportional to ROTI for weak scintillations and that the ratio ROTI/S_4 varies between 2 to 5 at Ancón, Peru. Using their own data set, Basu et al. (1999) similarly found that ROTI/S_4 varies between 2 to 10 at

Ascension Island. Li et al. (2007) reported the ratio of ROTI/S_4 varies between 0.3 and 6 in the Chinese low latitude region.

This study is the first which gives the characteristics of ionospheric scintillations observed on GPS at low latitudes over Vietnam. We used three receivers installed at PHUT (Hanoi), HUES (Hue) and HOCM (Ho Chi Minh City) during the period 2006-2014. Our study presents the climatology of scintillation and their directional occurrences. We considered the ratio between the ROTI and S_4 indices during the increasing phase of solar activity (2009 to 2011) in order to provide additional informations on the relationship between scintillation and ROTI at low-latitudes.

2. Data and method of analysis

We used scintillation data recorded by three GISTM receivers (GPS ionospheric scintillation and TEC monitors), installed in Vietnam in the framework of the scientific co-operation between the Institute of Geophysics (Vietnam) and University of Rennes 1 and National School of Telecommunication of Brest (France). Figure 1 shows the location of the stations and the GPS satellites paths at the level of the piercing points at the altitude of 400 km, on January 07, 2010. On this figure the magnetic equator calculated by the IGRF 2010 model is plotted by a line quasi parallel to the geographic equator at a latitude 7.5-8^{o}N.

The GSV4004 receiver measures the amplitude and the phase of the scintillation from the L1 frequency signal at a sampling rate of 50 Hz, and the ionospheric TEC from the L1 and L2 signals. In this paper, we use the S_4 index to study the characteristics of occurrence of ionospheric scintillations. The S_4 index is computed from the normalized standard deviation of raw signal intensity (S_{4T}) and for each 1-min period. The corrected S_4 index is computed by removing the

effects of ambient noise (S_{4No}), as follow (Rama Rao et al., 2006; Abadi et al., 2014):

$$S_4 = \sqrt{S_{4T}^2 - S_{4No}^2} \qquad (1)$$

However, S_4 calculated with this formula may still contain multipath effects, particularly at low elevation angles. In previous studies, to avoid multipath effects, there are two methods: 1) to remove the data at elevation angle lower than 40 degrees (Rama Rao et al., 2006; Li et al., 2007) and 2) to use a filter limit for separating multipath and ionospheric scintillation signal (Van Dierendonck and Hua, 2001; GSV GPS Silicon Valley, 2005; Beniguel and Adam, 2007; Romano et al., 2013; Abadi et al., 2014). In this study, we used the method of Van Dierendonck and Hua, (2001) and Abadi et al. (2014). Details on methodology can be found in Abadi et al. 2014. Following this technique, we defined the filter limit for the scintillation data of PHUT, HUES and HOCM stations as shown on figure 2. All scintillation data above the line are likely multipath effects, are excluded from the data analysis.

Figure 3 illustrates the difference between the unfiltered and filtered data. The maximum S_4 values of all visible satellites each minute are plotted according to the same color scale for PHUT, HUES and HOCM during March 2010. Figure 3a, 3b and 3c show the maximum S_4 values without filter for PHUT, HUES and HOCM, respectively. The dark region indicates that no there are data. The plots are very noisy because the same S_4 variation is repeated every day. These S_4 values are due to multipath effects. Figure 3d, 3e and 3f show the scintillations after filtering for an elevation angle higher than 10 degrees at PHUT, HUES and HOCM. The results show that the filtering removes all S_4 values associated with multipath effects.

The rate of change of the total electron content (ROT), computed from the differential carrier phase, can provide information on large scale irregularities of electron density. The TEC fluctuations are commonly characterized by the parameter ROTI, defined as the standard deviation of the rate of ROT, computed for each 1 or 5 minute time interval (Pi et al., 1997; Basu et al., 1999, Carrano and Groves, 2007). It is calculated as follows:

$$ROTI = \sqrt{\langle ROT^2 \rangle - \langle ROT \rangle^2} \qquad (2)$$

Where $ROT(t_j) = \frac{TEC(t_j) - TEC(t_{j-1})}{t_j - t_{j-1}}$, (3) in TECU/min.

TEC computed from the carrier phase observations L1 and L2 (*f1=1.57542 GHz, f2 = 1.22760 GHz*). This ROTI index can be used to indicate the presence of scintillation causing small-scale ionospheric irregularities in the equator region (Pi et al., 1997). In this study, the ROTI index is calculated for 5 minute running window.

3. Results and discussion

In this paper, we used all the data each minute at three stations for the period 2009 to 2014 at PHUT, and the period 2006 to 2011 at HUES and HOCM. We considered only the scintillation data with the S_4 index greater than 0.2 and an elevation angle higher then 10 degrees; in Vietnam the local time (LT) is equal to universal time (UT) plus 7.

3.1 Scintillation climatology in the Vietnam region

Figure 4 shows the seasonal variation of the occurrences of ionospheric scintillation at PHUT, HUES and HOCM during the period of study. The monthly variation of the F10.7 solar index from 2006 to 2014 is also plotted on figure 4.

The monthly probability of occurrence of scintillation was classified in two levels: the weak to moderate ($0.2 < S_4 < 0.6$) and the strong ($S_4 \geq 0.6$). The occurrence rate is calculated as the number of scintillation event (1 minute value) in each month divided by total possible values in one year during nighttime (from 6 pm to 6 am).

The results show that in each year the occurrence of scintillation depends on the month. The maximum of scintillation activity occurs during the equinox months and the minimum during summer and winter months in all stations. There are number of studies which reported seasonal occurrences of ionospheric irregularities over Southeast Asian region. Liu et al. (2015) analyzed the scintillations in Sanya (18.3° N, 109.6° E) from July 2004 to December 2012. They found a maximum of the scintillations at the equinoxes during the maximum of the sunspot cycle. They also observed daytime scintillations at the June solstice during the minimum of the sunspot cycle. Abadi et al. (2014) studied the scintillations at Bandung (6.9° S, 107.6° E) and Pontianak (0.02° S, 109.3° E), from January 2009 to December 2011. They observed a maximum of the scintillations at the equinox months. Recently, Kumar and Chen (2016) found the occurrence maximum of EPB at June solstice during the deep solar from 2007 to 2009. The model of Fejer et al. (2008) based on 5 years of ROCSAT satellite data, recorded from March 1999 to June 2004 shows that the vertical ExB drift present maximum varying with season and longitude sector. We know that this drift with its post sunset PRE is an essential parameter for the existence of scintillations. If we look at figure 6 of the model in Fejer et al; (2008) we see that for Vietnam which is located at +110° the maximum of the PRE is observed at the equinoxes. On the contrary at longitude around -60° the maximum of the PRE is observed in winter. At PHUT during of the maximum of the sunspot cycle 24 we observed the maximum of scintillations at equinox. At HUES and HOCM during the moderate and deep solar from 2006 to 2011, scintillation was observed rarely, however there is still the existence of maximum at equinoxes. Our results like Liu et al. (2015), Abadi et al. (2014) and this fact corresponds also to the model of Fejer et al. (2008).

We observe a gradual increase of scintillation activity, including both the weak-moderate and strong activities at PHUT from 2009 to 2014 and gradual decrease from 2006 to 2009. At HUES and HOCM, the increase of scintillation activity from 2009 to 2011 depends on the solar activity. Indeed during the minimum solar activity years 2008-2009, the scintillation activity is very weak. In 2010, the Sun entered in the ascending phase of solar sunspot cycle 24 and the scintillation activity increased in comparison with the previous years during the minimum phase of solar sunspot cycle 23 (from 2006 to 2007). The rate of occurrences of strong scintillations increases during the years of solar sunspot maximum at PHUT (2012, 2013 and 2014). To estimate the effect of solar activity on scintillation, we calculated the correlations between the monthly occurrence percentage of all S4 values and the solar flux (F10.7). We considered all the set of days (magnetically quiet days and magnetically disturbed days) to perform our statistical study for two reasons. The first reason is that over 75% of days are magnetic quiet days and this for all years. The second reason is that the magnetic activity can inhibit or reinforce scintillations (Li et al; 2008, Li et al., 2009, Carter 2014) and in the average its effects disappear. The correlation coefficients are 0.40 for PHUT during the periods 2009-2014, 0.52 for HUES and 0.67 for HOCM during the periods 2006-2011. The correlation is better near the magnetic equator than near the crests. The previous studies showed that the scintillation occurrence in the low-latitude region is almost associated with plasma bubble (Rama Rao et al., 2006; Saito et al., 2008; Abadi et al., 2014; Bhattacharyya et al., 2014). The scintillations are due to ionospheric irregularities generated at the equatorial region through RT plasma instability, which is considered as the primary mechanism responsible for the generation of plasma bubble. At low latitudes, the mapping of these irregularities through the magnetic field lines depends on the altitude reach by the irregularities. When these irregularities are mapped down to the equatorial anomaly crest region, where the ambient electron density is higher compared to the electron density at dip equatorial stations it give rise to strong scintillations

(Bhattacharya et al., 2014). Therefore, strong scintillations appear more near the anomaly crest and this is observed at PHUT located near the northern crest of the EIA. Morphology of plasma bubbles and ionospheric conditions near the crest are more complex than over the magnetic equator and that can explain the decrease of the correlation between the monthly percentage of occurrence of scintillation and the sunspot number, far from the magnetic equator. These correlations are worse than the correlations between the monthly mean TEC values and the sunspot number: ~0.88 at the crest of the EIA in the Southeast-Asian region (Le Huy et al., 2014). This can be understood because there is a direct relationship between the ionospheric electron density and solar activity, while the scintillation activity depends on more complicated ionospheric, magnetic and solar conditions.

Figure 5 shows the percentage of occurrences of scintillation activity as a function of local time and latitude for the period from 2009 to 2011, when there are the simultaneous data in three stations. We assume the altitude of 400km for the ionospheric pierce point. The percentage of occurrences of scintillation is shown by a color scale. The figure is divided in a grid with a pixel (1h x 0.5^o) corresponding to local time and geographic latitude for all the days. We observe the following features: 1) most of the ionospheric scintillations occur after sunset until pre-midnight (from 19h to 24h LT) 2) the scintillations are maximum at about 20 to 21h LT with a percentage occurrence up to 1.5% in some areas and 3) there are very few ionospheric scintillations during the post-midnight hours. These results also show that there is a concentration of scintillation activity in area from 15^o to 20^oN geographic latitudes (about 8^o to 13^oN magnetic latitudes), with a peak at about 16^oN geographic latitude (9^oN magnetic latitude). Le Huy et al., (2014) showed that the location of the monthly northern crest of the EIA in Vietnam region during 2006-2011 period vary between 17^o to 22^oN geographic latitudes (about 10^o to 15^oN magnetic latitudes). Therefore we can conclude that scintillation occurrences concentrate around the northern crest of the EIA. Some

previous studies also found the concentration of scintillation around the EIA (Valladares et al., 2004; Rama Rao et al., 2006). At the crest of the EIA there are large ionospheric densities and large gradients accompanied with the presence of small-scale irregularities during the post sunset hours. All these characteristics give rise to the generation of scintillation of the GPS signals.

3.2 Directional distribution

Figure 6 shows the occurrence rate of scintillation as a function of azimuth and elevation angles for the station PHUT for all the years. The elevation and azimuth variations are from 10^o to 90^o and from 0^o to 360^o, respectively. The percentage of occurrence of scintillations is divided by intervals of 10^o in elevation angles and 20^o in azimuth angles. From these plots, we can see clearly that the scintillations occur mainly at elevation angle 20^o-30^o in the southern sky (equatorward) of PHUT. During the maximum of solar sunspot activity years (2012, 2013 and 2014), the distributions of scintillations develop widely from the southern to northern sky of PHUT and from low to large elevation angle. Abadi et al. (2014) showed that the distribution of scintillations for Bandung, exhibits the highest concentration of occurrences at 20^o-30^o elevation angle in the northern sky (equatorward) of Bandung. The directional distribution of scintillation for PHUT (magnetic latitude 14.37^oN) is similar to the one for Bandung (magnetic latitude 17.5^oS), but in opposite direction because Bandung is in southern hemisphere.

Figure 7 shows the occurrence rate of scintillations as a function of azimuth and elevation angles for HUES during the period 2006-2011. The directional distribution of scintillation occurrences for HUES is different than the PHUT one. The scintillations occur less and are distributed in both the northern and the southern skies of HUES. These results show also that the distribution is much larger in the northern sky (poleward) than in the southern sky of HUES. In 2011,

the scintillation activity was enhanced with increasing solar sunspot activity. The sky plot shows that there is a larger distribution in both the southern sky (20^o-40^o and 320^o-340^o in azimuth) and the northern sky (180^o-220^o in azimuth) of HUES, at 30-40^o elevation angle.

Similarly, Figure 8 shows the result for HOCM during the period 2006-2011. The distribution of scintillation occurrences for HOCM is similar to HUES, the scintillations are distributed in both the northern and the southern sky of HOCM. The distribution is much larger in the northern sky (poleward) than in southern sky of HOCM. In the northern sky of HOCM, there is the large concentration of scintillations around 20^o-40^o and 320^o-340^o in azimuth (in the eastward and westward directions) and 20^o-40^o in elevation angle. In the southern sky of HOCM, scintillations occur mainly at 160^o-200^o in azimuth and at low elevation angle. Unlike HUES station, scintillation occurrences in the southern sky of HOCM concentrate at low elevation angle (less than 20^o). If we withdraw all the data below the 40^o elevation angle, as for previous studies, we can not get the directional distribution information of scintillation at HUES, HOCM and PHUT during low solar sunspot activity years because most of the scintillations occur at low elevation angle.

To explain the directional distribution of scintillations observed for all stations in Vietnam, we must consider several factors related to the scintillations. Figure 9 shows the yearly mean maps of the diurnal TEC in the Southeast Asia from 8 GPS stations in Vietnam and the Southeast Asian region (PHUT, HUES, HOCM, CUSV (13.7^{o}N, 100.5^{o}E), NTUS (1.4^{o}N, 103.7^{o}E), BAKO (6.5^{o}S, 106.9^{o}E) and XMIS (10.5^{o}S, 105.7^{o}E)). Figure 9 shows that the northern crest is located around 20-21^{o}N during 2006-2014 and that PHUT is located under or at the outer edge of the anomaly crest. The enhancement in scintillation occurrences in the southern sky of PHUT may be explained by the location of EIA crest and the latitudinal extent of plasma bubbles. During the years of low solar activity

(from 2006 to 2010), the magnitude and extension of both anomaly crests are low, there are low ambient electron density and low electron density gradient and as a consequence weak scintillations. Otherwise, the latitudinal extension of plasma bubbles to the anomaly crest region will cause that TEC falls more sharply to the mid latitudes than towards the equator. So the population of scintillation events is more in the inner edge of the anomaly crest compared to that at the outer edge (Rama Rao et al., 2006; Cervera and Thomas, 2006). During years of high solar sunspot activity (from 2011 to 2014), the magnitude of anomaly crest enhances and extends poleward. Then the latitudinal extent of plasma bubbles to the anomaly crest region causes large plasma depletions causing strong scintillation activity on the GPS signals. We can see that the ionospheric scintillation distributions develop from the southern to northern sky of Hanoi during this time.

For HUES, situated between the northern anomaly crest and the magnetic equator, the enhancement in scintillation occurrences in the northern sky of HUES can be explained by the location of northern EIA crest. However, the location of EIA crest cannot explain the second peak in scintillation occurrences in the southern sky of HUES and the maximum occurrences at 30^o-40^o elevation angle for HUES because the scintillation occurrences at 30^o-40^o are larger than those at low elevation angle. The previous studies for the low latitude regions have reported the enhancement in scintillation occurrences in the direction of the field-aligned (Anderson and Straus, 2005; Abadi et al., 2014). Abadi et al. (2014) showed that the magnetic field-aligned irregularities are the causes of scintillations at 20^o-30^o elevation angles in the northern sky of Pontianak (magnetic latitude 8.9^oS). Pontaniak is close to the magnetic conjugate point of HUES. So the concentration of occurrences at the 30^o-40^o elevation angles in the southern sky of HUES seems to be associated with field-aligned plasma irregularities. For HOCM, situated outside of the anomaly crest and close to the magnetic equator, the enhancement in scintillation occurrences in the northern sky of HOCM can be

explained by the location of EIA northern crest. The second peak of scintillation in the southern sky of HOCM in low elevation angles region can be explain by slant path length through the EIA southern crest region.

3.3 Correlation between amplitude scintillation and TEC fluctuation

The ROTI provides information about the presence of ionospheric irregularities at the scale of few kilometers or more, while S_4 is related to the presence of ionospheric irregularities at the scale-size of the first Fresnel zone (~400m). The combined used of S_4 and ROTI allows explaining the evolution of turbulence scales in the ionospheric physical mechanisms. The relationship between the amplitude of scintillations and the TEC fluctuations has been explored in previous studies (Basu et al., 1999; Beach and Kintner, 1999; Xu et al., 2007; Li et al., 2007; Carrano and Groves, 2007).

In this study, the ROTI values are calculated for a 5 minutes running window. We consider the relation of ROTI and S_4 each minute; it might provide a correlation more real compared with the averaged over the 5 minutes S_4 in previous studies (Basu et al., 1999; Xu et al., 2007). To compare S_4 index with ROTI value, we select the ROTI values with ionospheric scintillation activity ($S_4 \geq 0.2$) during the nighttime for the period of 2009-2011. Basu et al. (1999) suggested that there are two major ROTI and S_4 structures, one during the pre-midnight hours and the other during the post-midnight period. Then, in this case, we consider the correlation analysis for different local time periods, one for pre-midnight hours (18-24LT) and the other one for post-midnight hours (00-06LT). For each valid sample, the recorded azimuth and elevation angle are used to compute the IPP latitude and longitude, with assumed the altitude at 400 km. The longitude is used to evaluate the local time at the IPP. We use the local time at IPP, but not the local time of the receiver because the IPP distributes widely in the sky plots. Figure 10 illustrates scatter plots of all 1-min values of ROTI and S_4

with elevation angle above 10° during 2009-2011 for PHUT, HUES and HOCM. There is a strong scatter in the figure due to the fact that data are not averaged during a long time interval. The linear regression line in the scatter plot shows the correlation trend of ROTI and S_4. Table 1 shows the correlation value of ROTI and S_4 during the pre-midnight and the post-midnight period for each station. We find that the correlation between ROTI and S_4 is low and the correlation in the post-midnight hours is higher than the correlation in the pre-midnight hours for all stations. The irregularities affecting S_4 are more concentrated in the pre-midnight hours than in the post-midnight hours. These results can be explained by the co-existence of large and small-scale irregularities in equatorial irregularity structure during the pre-midnight period and the decay of small Fresnel scale irregularities due to enhancement of diffusion in the post-midnight period (Basu et al., 1978, 1999). Normally, ROTI is more weighted towards large-scale irregularities, while S_4 is weighted toward small-scale irregularities. The smaller correlation in the pre-midnight period highlights the fact that the existence of many scale size of irregularities in the equatorial region cause the strong fluctuations in the observations of ROTI and S_4. The higher correlation in the post-midnight hours shows that the decay of the small-scale irregularities and the existence of larger-scale irregularities may produce week scintillations on an L-band signal. We also find that the correlation between ROTI and S_4 is higher at PHUT (under EIA) than at HOCM (near magnetic equator). This may be relative with the evolution of intermediate-scale irregularities within an EPB when it grows up and emerges into the topside ionosphere. The top side irregularities would map down to a region near the EIA crest along geomagnetic field lines, where there is a higher ambient electron density. It would result in stronger irregularities at region near the EIA crest than the equatorial F region. Recently, Bhattacharya et al. (2014) found that the shortest of irregularities scale size obtained at the dip equator would still be much larger than that obtained near the anomaly crest. Xu et al. (2007) used the data with elevation angles above 30° from Wuhan station (magnetic latitude

19.4°N) during period from May 2003 to December 2004 and estimated a very high correlation coefficient (about 0.97) between ROTI and S_4. Whereas Basu et al. (1999) indicated a high scatter with a low correlation coefficient between ROTI and S_4 at Ascension Island (magnetic latitude 16°S). The results in this study are in agreement with the observations of Basu et al. (1999) during Feb-Mar 1998 at Ascension Island.

Figure 11 illustrates the variations of the ratio of ROTI/S_4 from one satellite to another, for the three stations. In all stations, the ratios ROTI/S_4 are mostly less than 8 for all satellites, but some satellites give the ratio ROTI/S_4 larger than 8. When all satellites are considered, the ratio of ROTI/S_4 varies between 1 and 7 for PHUT, between 0.3 and 6 for HUES and between 0.7 and 6 for HOCM. The ratio of ROTI/S_4 is almost greater than 1 at PHUT; this fact probably indicates that the values of S_4 are very often detected with large-scale irregularities. The percentage of the ratio of ROTI/S_4 less than one at HUES and HOCM is about 18.2% and 12.5%, respectively. The observed values of the ROTI/S_4 ratio less than one show that the existence of small-scale density fluctuations causing the fluctuations in the S_4 index are larger than large-scale density fluctuations causing ROTI. By using GPS TEC data obtained from the GPS receivers at Ascension Island, Basu et al. (1999) found that ROTI/S_4 varies between 2 and 10. Beach and Kintner, (1999) found that ROTI/S_4 varies between 2 and 5 at Ancon, Peru. Li et al. (2007) found that ROTI/S_4 varies between 0.3 and 6 at Sanya, China. Compare with these previous studies, the ratio of ROTI/S_4 for PHUT (magnetic latitude 14.37°N) is similar to the observations of Basu et al. (1999) for Ascension Island (magnetic latitude 16.0°S), and the ratio of ROTI/S_4 for HUES (magnetic latitude 9.45°N) and HOCM (magnetic latitude 3.34°N) is similar to the observations at Sanya (magnetic latitude 7.04°N) by Li et al. (2007). The quantitative relationship between ROTI and S_4 varies considerably due to variations of the projection satellite velocity in the ionosphere and the ionospheric irregularity drift (Basu et

al., 1999). For different GPS satellites with varying satellite trajectories, the ionospheric projection of the satellite velocity is different, even for the same irregularity drifts, so the scale-length of ROTI for different satellites will be different. In this study, we used a data set as long as possible to provide additional information about the relationship between amplitude of scintillations and ROTI in the equatorial region.

4. Conclusion

Using the continuous data from three GSV4004 receivers at PHUT, HUES and HOCM in Vietnam during the period 2006-2014, we present the climatology, the directional analysis of scintillation occurrences and the estimate of the correlation between ROTI and S_4 in each station. The main result can be summarized as following.

- Over Vietnam region, the distribution of scintillation occurrences is dominant during the pre-midnight hours and around the northern crest of EIA, from the 15^oN to 20^oN geographic latitudes with maximum at about 16^oN. The scintillation activity is maximal during equinox months for all the years (2006-2014) and depends on solar activity. The correlations between the monthly percentage scintillation occurrence and sunspot number are of 0.39, 0.48 and 0.61 for PHUT, HUES and HOCM respectively.

- The result obtained from directional analyzes in each station showed that: scintillations occur mainly in low elevation angle region (less then 40^o). There is a concentration of scintillation occurrences in the southern sky of PHUT which extend to northern sky during the maximum solar sunspot activity. For HUES and HOCM, there are two peaks of scintillation occurrences in the northern sky and the southern sky with a higher distribution in the northern sky. These enhancements of scintillation occurrences can be explained by the location of EIA crest and the latitudinal extent of plasma bubbles. However, the second peak in scintillation occurrence in the southern sky of HUES and the maximum

occurrences at the 30^o-40^o elevation angles for HUES seems to be associated with field-aligned plasma irregularities.

- We found that the correlation between ROTI and S_4 is low but larger at PHUT (under EIA) than HOCM (near equator). We also found a better correlation during the post-midnight hours than during the pre-midnight hours, for all station. When all satellites are considered during the period of 2009-2011, the range of variation of ROTI/S_4 is from 1 to 7 for PHUT, from 0.3 to 6 for HUES and from 0.7 to 6 for HOCM.

We analyzed a lot of data and thus formed a scintillation database in Vietnam. This first work presents the morphological characteristics of scintillations in Vietnam. Further studies will be carried out in the future, notably to understand the relations between scintillations and magnetic activity or to link scintillations with other physical processes such as gravity waves or planetary waves.

Acknowledgements

The GPS receivers at PHUT, HUES and HOCM have been installed in frame of the international project of scientific cooperation between the National Centre for Scientific research of French and the Vietnam Academy of Science and Technology. The authors thank the IGS Community for making available GNSS data; the F10.7cm flux data is taken from http://lasp.colorado.edu/lisird/tss/noaa_radio_flux.html. We would like to thank S. Saito for giving valuable comments. This research has been supported by the research project of the Vietnam Academy of Science and Technology (No. VAST01.02/15-16).

References

Abadi P., Saito S., and Srigutomo W., 2014: Low-latitude scintillation occurrences around the equatorial anomaly crest over Indonesia, *Ann. Geophys.*, **32**, 7-17.

Alfonsi L., L. Spogli, M. Pezzopane, V. Romano, E. Zuccheretti, G. De Franceschi, M. A. Cabrera, and R. G. Ezquer, 2013: Comparative analysis of spread-F signature and GPS scintillation occurrences at Tucumán, Argentina, *J. Geophys. Res.*, **118**, 4483–4502, doi:10.1002/jgra.50378.

Anderson P. C. and P. R. Straus, 2005: Magnetic field orientation control of GPS occultation observations of equatorial scintillation, *Geophys. Res. Lett.*, Vol.**32**, L21107:1-4, doi:10.1029/2005GL023781.

Basu, S., S. Basu, J. Aarons, J.P. McClure, and M.D. Cousins, 1978: On the coexistence of kilometer- and meter-scale irregularities in the nighttime equatorial F region, *J. Geophys. Res.*, **83** (A9), pp. 4219 - 4226.

Basu S., Groves K.M., Quinn J.M. and Doherty P., 1999: A comparision of TEC fluctuations and scintillations at Ascension Island, *Journal of Atmos. And Solar-Terrestrial Phys.*, Vol. **61**, 1219-1226.

Basu, S. and S. Basu, 1981: Equatorial scintillations, *A review Journal of Atmospheric and Terrestrial Physics*, vol. **43**, 473-489.

Beach T. L and Kintner M.P., 1999: Simultaneous Global Positioning System observations of equatorial scintillations and total electron content fluctuation, *J. Geophysc. Res.*, Vol. **104**, N.A10, 22553-22565.

Beniguel Y., Y., Romano, V., Alfonsi, L., Aquino, M., Bourdillon, A., Cannon, P., De Franceschi, G., Dubey, S., Forte, B., Gherm, V., Jakowski, N., Materassi, M., Noack, T., Pozoga, M., Rogers, N., Spalla, P., Strangeways, H. J., Warrington, E. M., Wernik, A., Wilken, V., and Zernov, N., 2009: Ionospheric scintillation monitoring and modelling, *Ann. Geophys.*, **52**, 391–416.

Beniguel Y., and Adam JP, 2007: Ionosphere Scintillation and their Effect on the Positioning Errors, *Proceeding of 1st Colloquium Scientific and Fundamental Aspects of the Galileo Programme*, Toulouse, October, 1-4,7p.

Bhattacharyya A., Kakad B., S. Sripathi, K. Jeeva, and K. U. Nair, 2014: Development of intermediate scale structure near the peak of the F region within an equatorial plasma bubble, *J. Geophys. Res*., **119**, 3066-3076.

Carrano C. S., and Groves K. M., 2007: TEC Gradients and Fluctuations at Low latitudes Measured with High Data Rate GPS Receivers, *ION 63rd Annual Meeting*, Cambridge, MA, 156-163.

Carter B. A., Retterer J. M., Yizengaw E., Groves K., Caton R., McNamara L., Bridgwood C., Francis M., Terkildsen M., Norman R., and K. Zhang 2014: Geomagnetic control of equatorial plasma bubble activity modeled by the TIEGCM with Kp, *Geophys. Res. Lett., 41, 5331–5339.*

Cervera M. A. and R. M. Thomas, 2006: Latitudinal and temporal variation of equatorial ionospheric irregularities determined from GPS scintillation observations, *Ann.Geophys.*, N.**24**, 3329-3341.

Fejer B.G., Scherlies, L., de Paula, E.R., 1999: Effects of the vertical plasma drift velocity on the generation and evolution of equatorial spread F, *J. Geophys. Res*. **104** (A9), 19,859–19,869.

Fejer B.G., John W. Jensen, and Shin-Yi Su, 2008: Quiet time equatorial F region vertical plasma drift model derived from ROCSAT-1 observations, *J. Geophys. Res*. **113**, A05304, doi:10.1029/2007JA012801.

GSV GPS Silicon Valley, 2005: GSV4004/GSV4004A – GPS Ionospheric Scintillation & TEC Monitor, USER'S MANUAL.

Huang L., J. Wang , Y. Jiang, Z. Chen, and K. Zhao, 2014: A study of GPS ionospheric scintillations observed at Shenzhen, *Advances in Space Research*, **54**, 2208–2217.

Kelley, M., 2009: The Earth's Ionosphere: Plasma Physics and Electrodynamics, eBook ISBN: 9780080916576, *Academic Press*, **Vol. 96**, 2nd Edition, Elsevier, New-York.

Kumar S. and Chen W., 2016: Remote sensing of ionospheric plasma bubbles using GPS/GNSS, Proceedings of 2016 International Conference on Localization and GNSS (ICL-GNSS) Barcelona, June 28-30, 2016, 2016 IEEE, 5p.

Le Huy M., C. Amory-Mazaudier, R. Fleury, A. Bourdillon, P. Lassudrie-Duchesne, L. Tran Thi, T. Nguyen Chien and T. Nguyen Ha, P. Vila, 2014 : Time variations of the total electron content in the Southeast Asian equatorial ionization anomaly for the period 2006-2011, *Advances in Space Research*, **54**, 355-368.

Li G, Ning B, and Yuan H., 2007: Analysis of ionospheric scintillation spectra and TEC in the Chinese low latitude region, *Earth Planets Space*, **59**, 279-285.

Li G., B. Ning, B. Zhao, L.Liu, J.Y. Liu, K. Yumoto, 2008: Effects of geomagnetic storm on GPS ionospheric scintillations at Sanya, *Journal of Atmos. And Solar-Terrestrial Phys.*, **70**, 1034–1045.

Li G. , B. Ning, L. Liu, W. Wan, and J. Y. Liu, 2009: Effect of magnetic activity on plasma bubbles over equatorial and low-latitude regions in East Asia, *Ann. Geophys.*, **27**, 303–312.

Liu K., Li G., Ning B., Hu L., and Li H., 2015: Statistical characteristics of low-latitude ionospheric scintillation over China, *Advances in Space Research*, **55**, 1356–1365.

Maruyama T., 2002: Ionospheric Irregularities, *Journal of the Communications Research Laboratory*, Vol.**49**, No.3, 163-178.

Pi X., Mannucci A. J., Lindqwister U. J., and Ho. C. M., 1997: Monitoring of global ionospheric irregularities using the worldwide GPS network, *Geophys. Res. Lett.*, Vol.**24**, N. 18, 2283-2286.

Rama Rao, P. V. S., Gopi Krishna, S., Niranjan, and Prasad, D. S. V. V. D, 2006: Study of spatial and temporal characteristics of L-band scintillation over the Indian low latitude region and their possible effects on GPS navigation, *Ann. Geophys.*, **24**, 1567-1580.

Romano V., L. Spogli, M. Aquino, A. Dodson, C. Hancock, B. Forte, 2013: GNSS station characterisation for ionospheric scintillation applications, *Advances in Space Research*, **52**, 1237-1246.

Saito S., Maruyama T., Ishii M., Kubota M., Ma G., Chen Y., Li J., Duyen C. H., Truong T. L., 2008: Observation of small to large scale ionospheric irregularities associated with plasma bubbles with a transequatorial HF propagation experiment and spaced GPS receivers, *J. Geophys. Res.*, V.**113**, A12313:1-10.

Spogli, L., Alfonsi, L., De Franceschi, G., Romano, V., Aquino, M.H.O., Dodson, A, 2009: Climatology of GPS ionospheric scintillations over high and mid-latitude European regions. *Ann. Geophys.* **27**, 3429–3437.

Tsunoda, R.T., 1980. Backscatter measurements of 11 cm equatorial spread F irregularities, *Geophys. Res. Lett.,* **7**, 848-850.

Valladares C. E., Villalobos J., Sheehan R., and Hagan M.P., 2004: Latitudinal extension of low laititude scintillations measured with a network of GPS receivers, *Ann. Geophys.*, **22**, 3155-3175.

Van Dierendonck A. J. and Hua Q., 2001: Measuring ionospheric scintillation effects from GPS signals, *Proceedings of the 57th Annual Meeting of the Institute of Navigation*, pp. 391–396.

Yeh K. C. and Chao-Han Liu, 1982: Radio wave scintillation in the ionosphere, *Proc. IEEE*, **70** (4), 324-358.

Xu J. S., Zhu J., and Li L., 2007: Effects of a major storm on GPS amplitude scintillations and phase fluctuations at Wuhan in China, *Advances in Space Research*, N.39, 1318-1324.

Table Caption

Table 1: The correlation between ROTI and S_4 during the pre-midnight and the post-midnight period.

Figure caption

Figure 1, Locations of GPS receiver stations in Vietnam and GPS satellite paths at the ionospheric piercing point at PHUT, at HUES and at HOCM on the 07th January 2010.

Figure 2, The filter limit of multipath effected data for PHUT, HUES and HOCM.

Figure 3, The differences between data analysis without filter for (a) PHUT, (b) HUES and (c) HOCM data and with filter for (d) PHUT, (e) HUES and (f) HOCM data during March 2010.

Figure 4, Monthly variation of the F10.7 index and the scintillation occurrences at PHUT from 2009 to 2014, at HUES and HOCM from 2006 to 2011.

Figure 5. Temporal and spatial of variation of the percentage occurrence of scintillation activity over Vietnam region for the period from 2009 to 2011.

Figure 6. The directional distribution of scintillations observed from PHUT station during 2009 - 2014.

Figure 7. The directional distribution of scintillations observed from HUES station during 2006 - 2011.

Figure 8. The directional distribution of scintillations observed from HOCM station during 2006 - 2011.

Figure 9, Time and latitudinal yearly mean TEC maps in the Southeast Asian for the 2006-2014 period. Contour interval: 5 TECu. Thick solid lines: 1- latitude of PHUT, 2- latitude of HUES and 3- latitude of HOCM.

Figure 10. Scatter plot of ROTI over S_4 (dot) for pre-midnight (18-24 LT) and post-midnight (0-6 LT) at PHUT, HUES, and HOCM, respectively.

Figure 11, The ratio of ROTI/S_4 for each visible satellite at PHUT, HUES and HOCM.

Table 1: The correlation between ROTI and S_4 during the pre-midnight and the post-midnight period.

Stations	Correlation coefficients The pre-midnight	Correlation coefficients The post-midnight
PHUT	0.49	0.52
HUES	0.34	0.38
HOCM	0.26	0.29

Figure 1

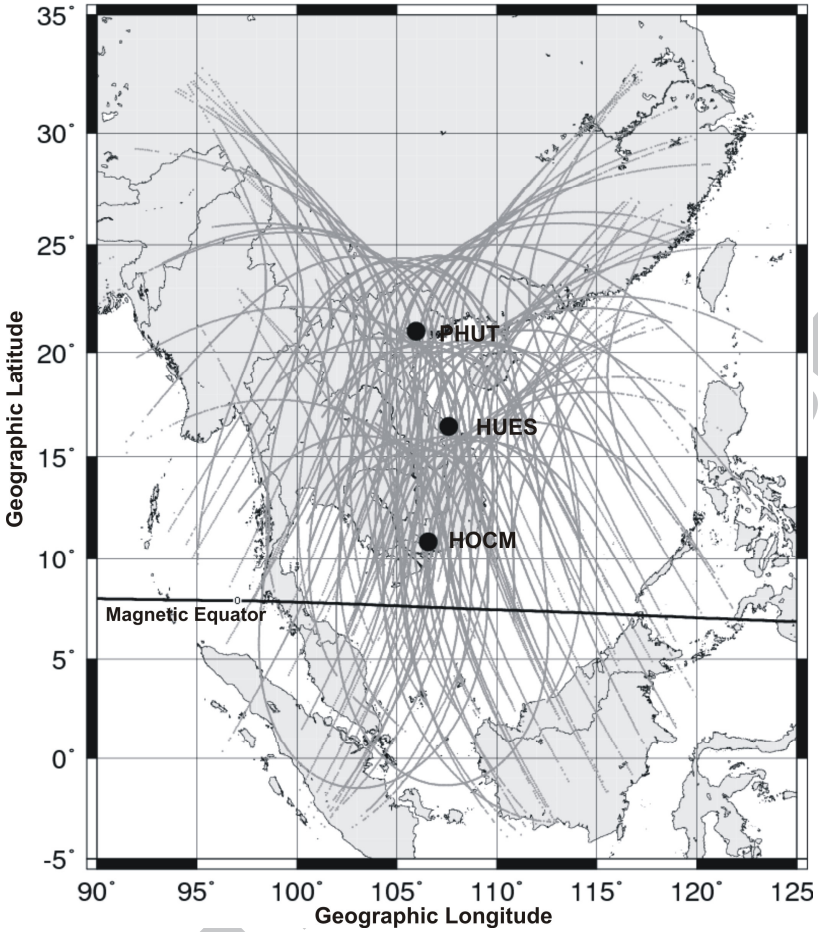

Figure 2

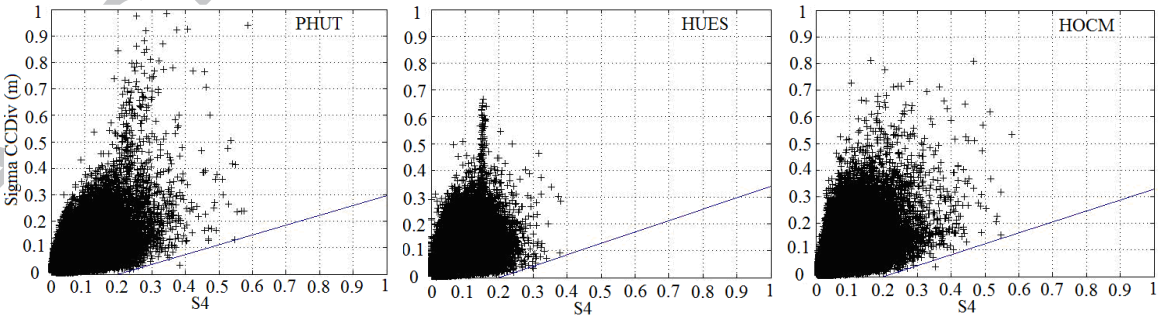

Figure 3

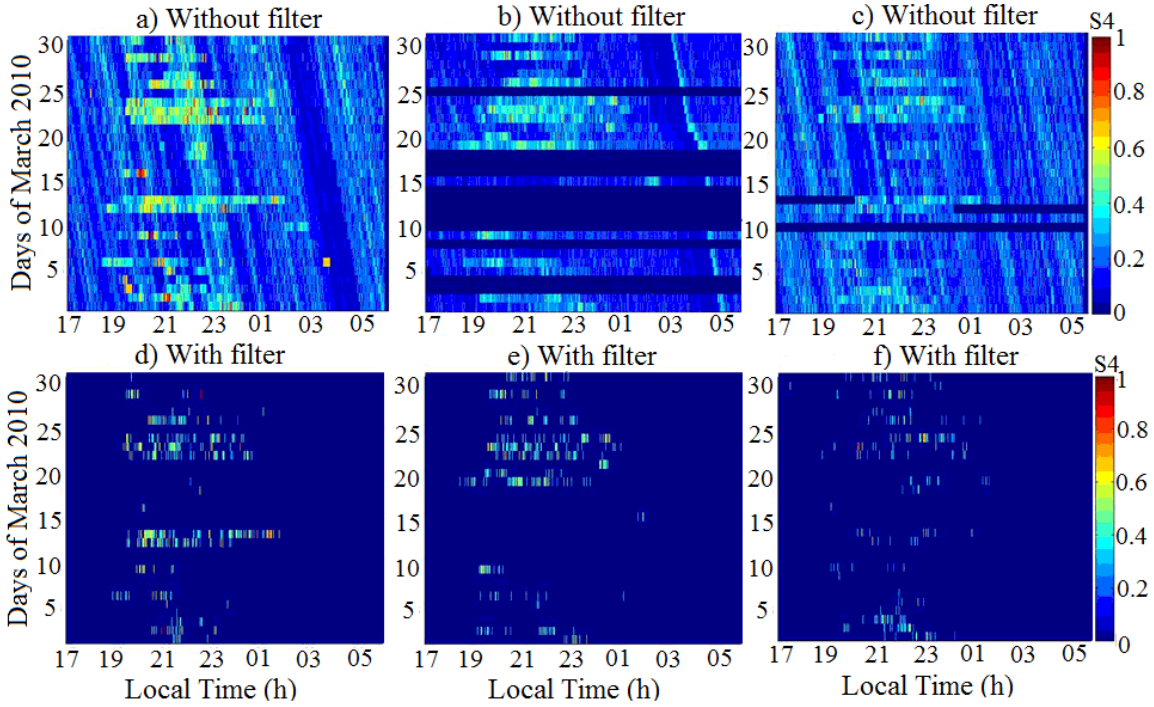

Figure 4

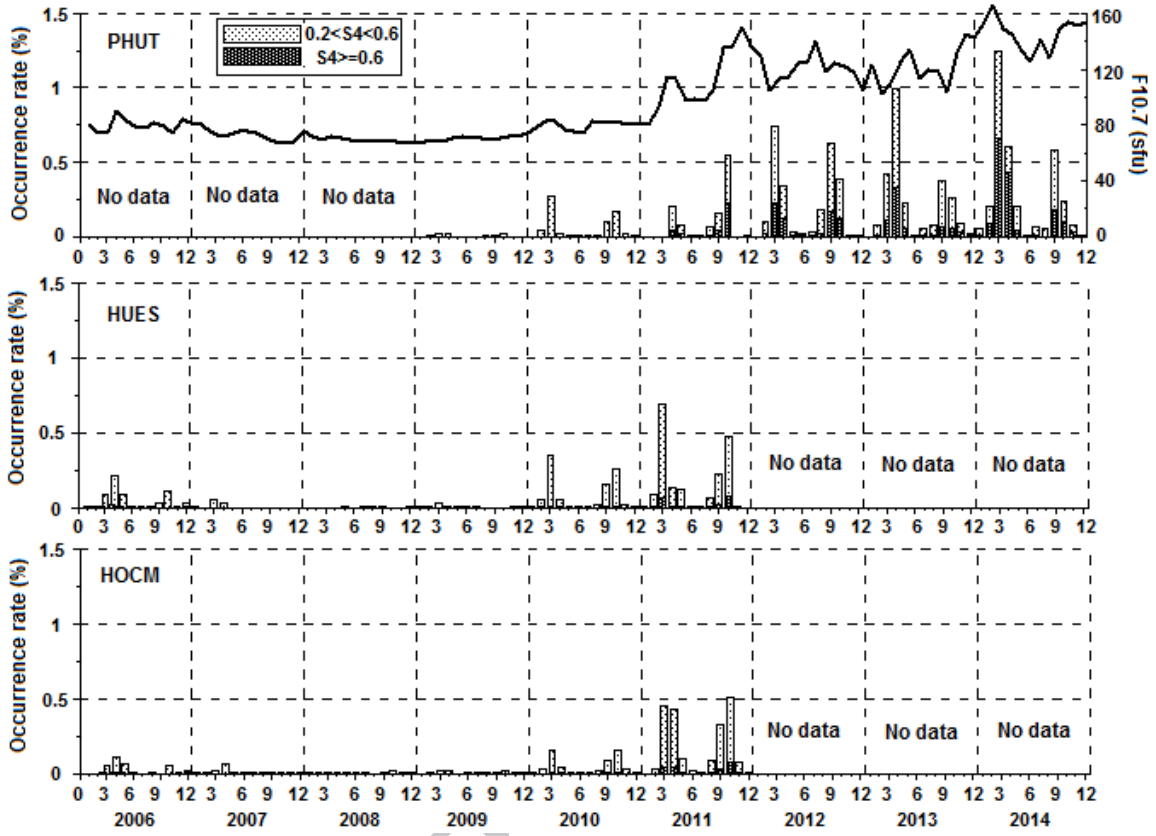

Figure 5

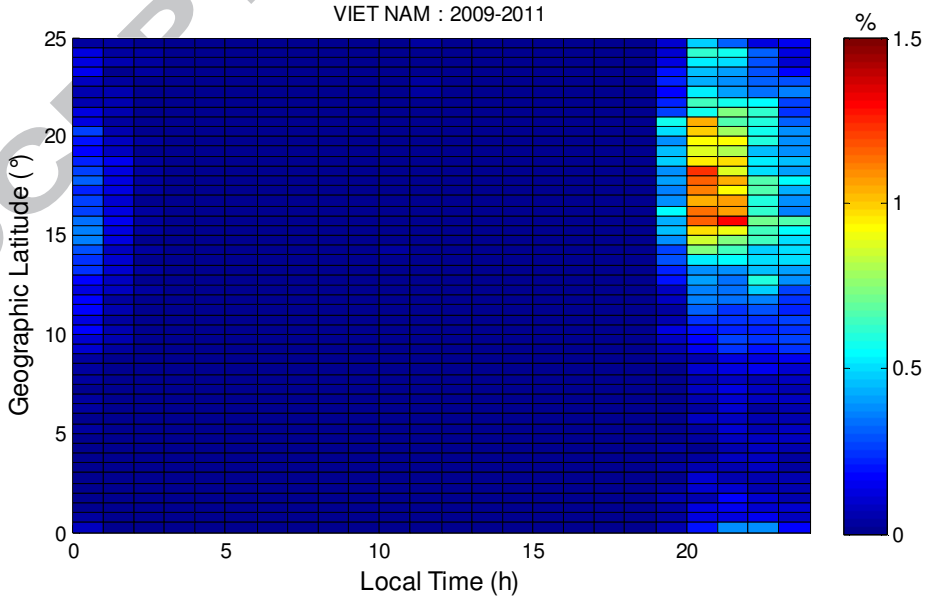

Figure 6

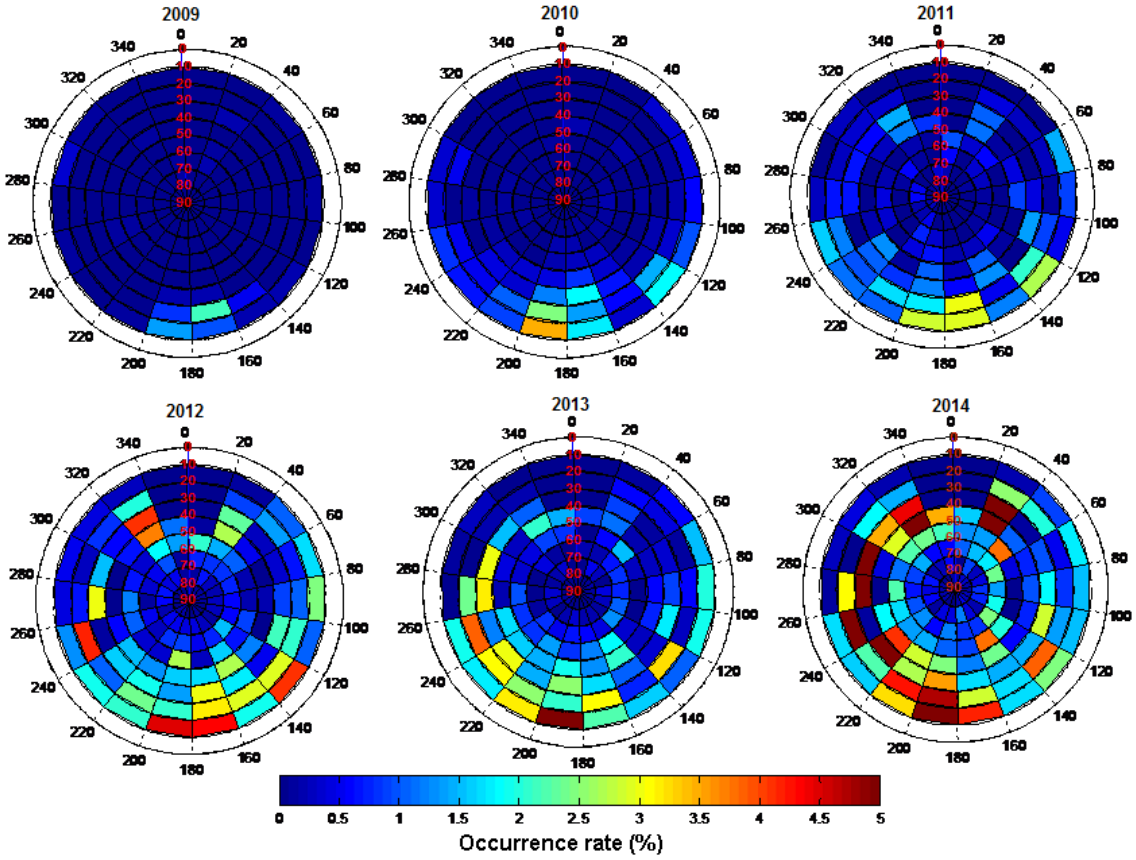

Figure 7

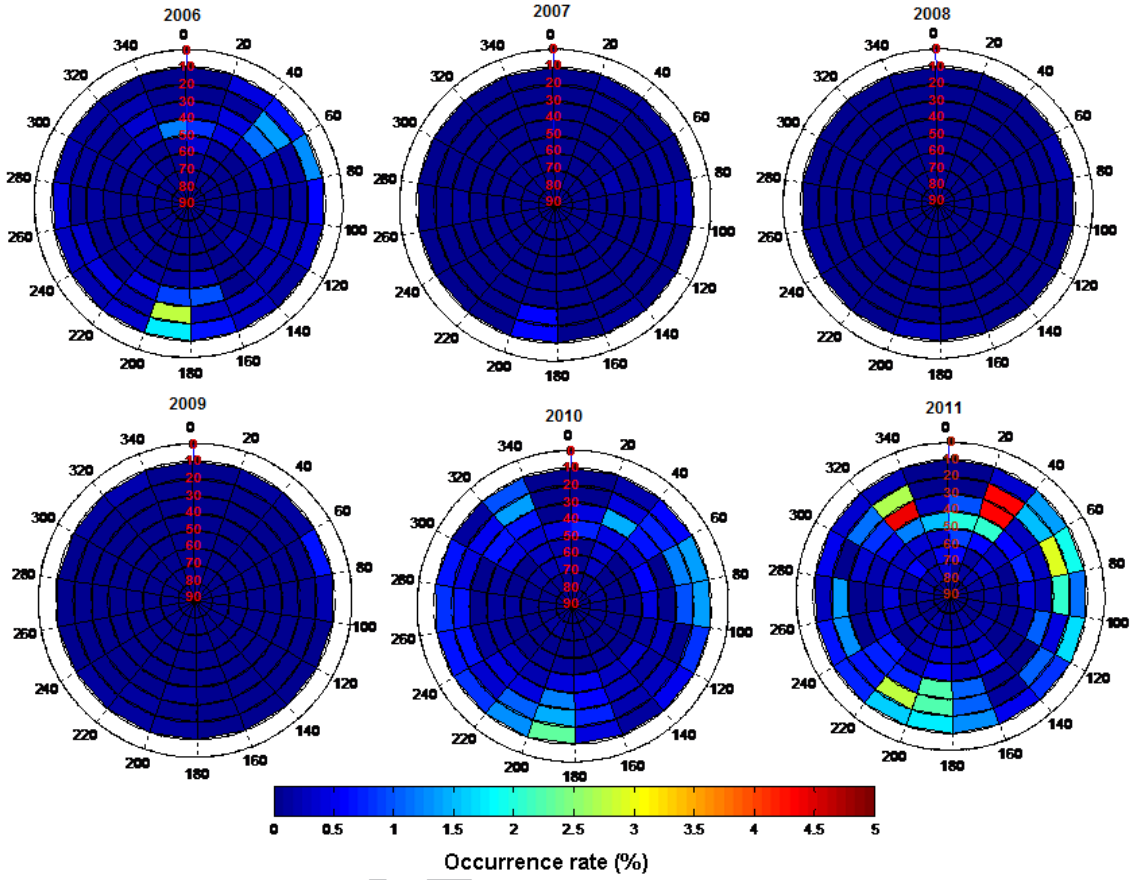

Figure 8

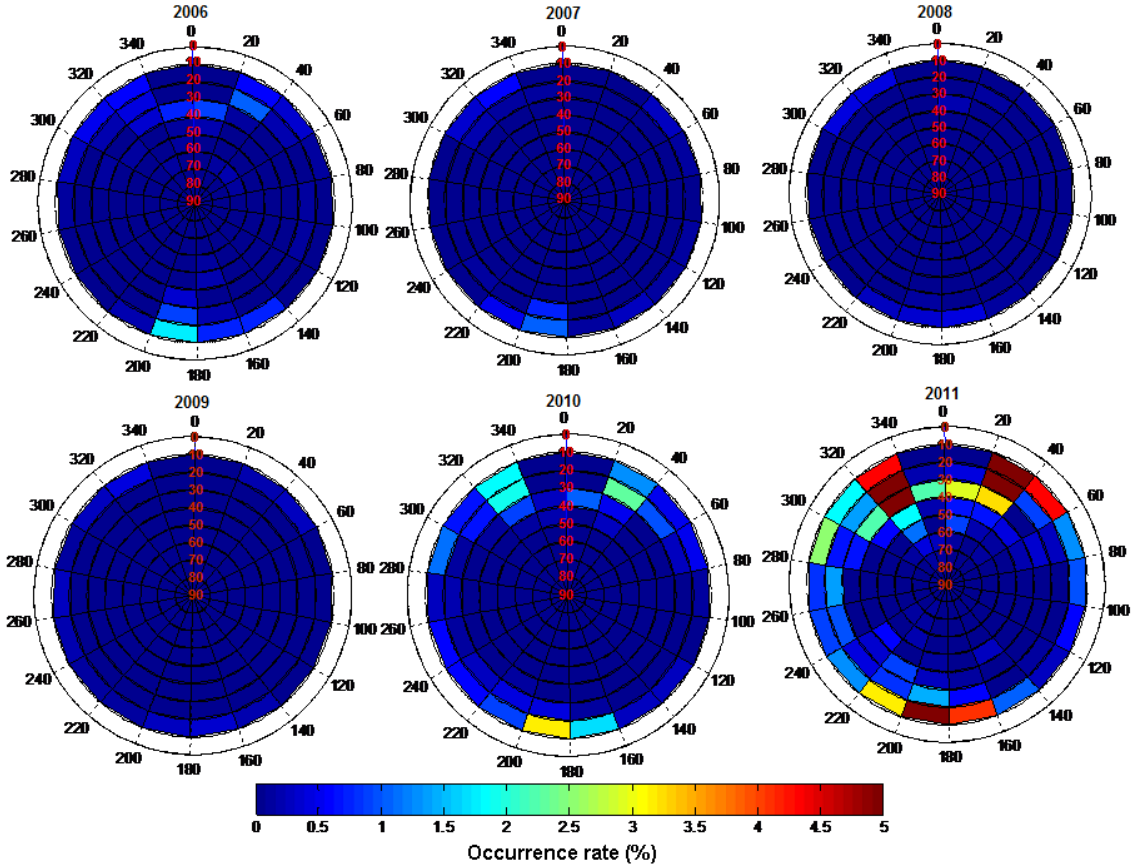

Figure 9

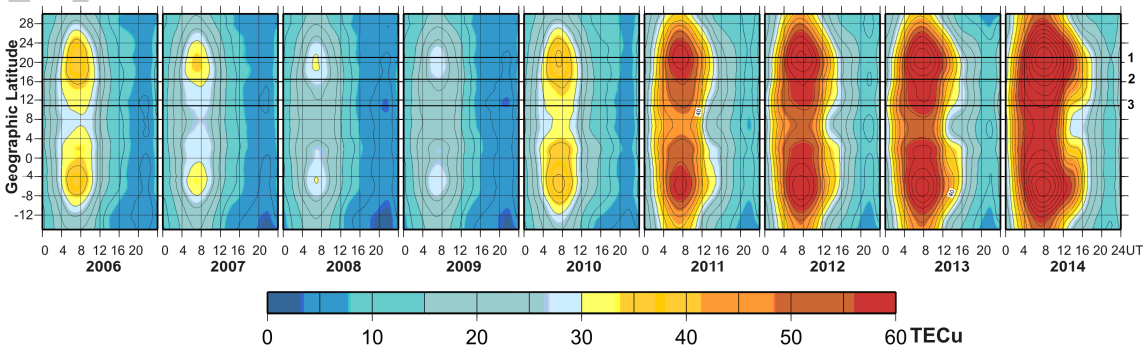

Figure 10

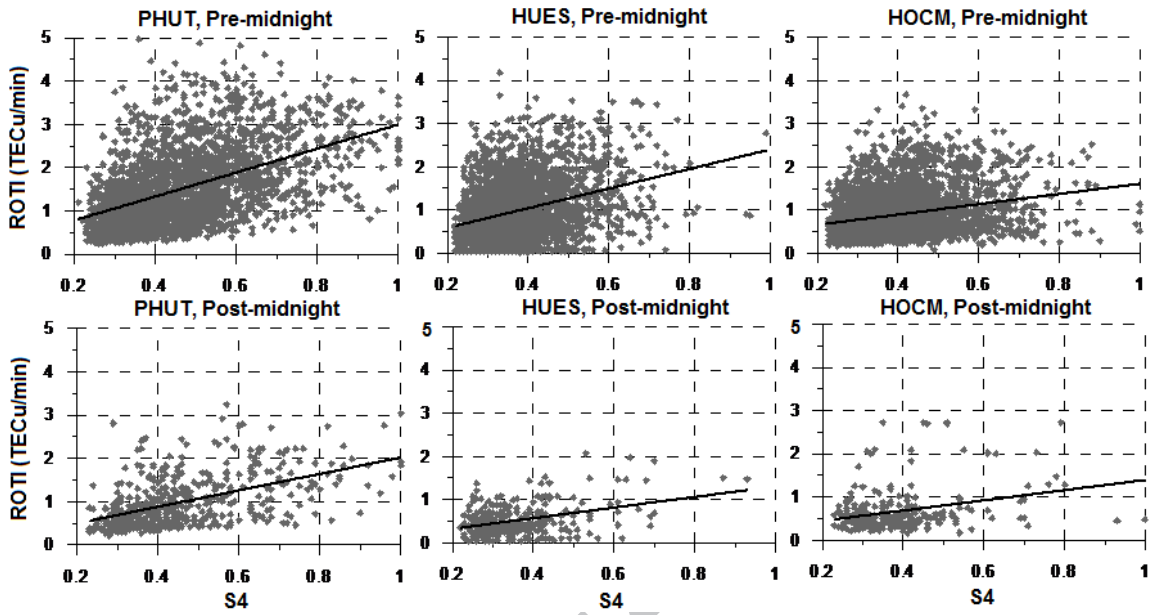

Figure 11